

October 31, 2002

Fermi surface evolution and collapse of the Mott pseudogap in $\text{Nd}_{2-x}\text{Ce}_x\text{CuO}_{4\pm\delta}$

C. Kusko

Northeastern University

R. S. Markiewicz

Northeastern University

M. Lindroos

Northeastern University

A. Bansil

Northeastern University

Recommended Citation

Kusko, C.; Markiewicz, R. S.; Lindroos, M.; and Bansil, A., "Fermi surface evolution and collapse of the Mott pseudogap in $\text{Nd}_{2-x}\text{Ce}_x\text{CuO}_{4\pm\delta}$ " (2002). *Physics Faculty Publications*. Paper 384.

Fermi surface evolution and collapse of the Mott pseudogap in $\text{Nd}_{2-x}\text{Ce}_x\text{CuO}_{4\pm\delta}$

C. Kusko,¹ R. S. Markiewicz,¹ M. Lindroos,^{1,2} and A. Bansil¹

¹Physics Department, Northeastern University, Boston, Massachusetts 02115

²Institute of Physics, Tampere University of Technology, 33101 Tampere, Finland

(Received 29 December 2001; published 31 October 2002)

Fermi surface (FS) maps and spectral intensities obtained recently in $\text{Nd}_{2-x}\text{Ce}_x\text{CuO}_{4\pm\delta}$ via high resolution ARPES measurements are analyzed using mean-field Hartree Fock and self-consistent renormalization computations within the framework of the one-band $t-t'-t''-U$ Hubbard model Hamiltonian. We show that the remarkable observed crossover of the FS from small to large sheets reflects a reduction in the value of the effective Hubbard U with increasing electron doping and the collapse of the correlation induced Mott pseudogap just above optimal doping.

DOI: 10.1103/PhysRevB.66.140513

PACS number(s): 74.25.Jb, 71.18.+y, 74.72.-h, 79.60.Bm

The $\text{Nd}_{2-x}\text{Ce}_x\text{CuO}_{4\pm\delta}$ (NCCO) high- T_c superconductor offers unique opportunities for investigating electron correlation effects in the cuprates. The reason is that the doped electrons in NCCO occupy states *above* the correlation induced gap (or more properly the pseudogap) in the electronic spectrum of the half-filled parent insulating compound. In sharp contrast, hole-doping involves states lying *below* the gap. In this connection, a recent angle-resolved photoemission (ARPES) study of NCCO (Ref. 1) reveals a remarkable crossover from small Fermi surface (FS) pockets near half-filling to a large three-pieced FS around optimal doping. This article examines the implications of the aforementioned ARPES results with respect to fundamental correlation effects in the cuprates.

Our analysis proceeds within the framework of the one-band² Hubbard Hamiltonian with hopping parameters t , t' , t'' and the on-site repulsive interaction U , where we have carried out extensive mean field (MF) Hartree Fock as well as self-consistent renormalization (SCR) (Refs. 3,4) computations. Highlights of the new results reported here are as follows. We show that the experimentally observed evolution of the FS of NCCO requires a decreasing value of effective U with increasing electron doping. In particular, the Mott pseudogap in the electronic spectrum is found to collapse around optimal doping as the staggered magnetization goes to zero and the $T=0$ Neel ordered state terminates, yielding a quantum critical point (QCP). We emphasize that much of the existing literature on electron-doped cuprates invokes $t-J$ models which assume a large, doping-independent U . The present results indicate that $t-J$ models are intrinsically limited for describing the electron-doped cuprates and that the use of $t-U$ models is essential. Finally, we have carried out extensive first-principles simulations of photointensities in order to ascertain that the key spectral features discussed in this article (e.g., growth of the $(\pi/2, \pi/2)$ centered *hole* orbit with doping) are genuine correlations effects beyond the conventional LDA framework and are not related to the energy and k dependencies of the ARPES matrix element.⁵

We set the stage for our discussion by summarizing some relevant results of our SCR and MF calculations. (The SCR theory which includes fluctuations is of course more accurate.) For the 2D $t-t'-t''-U$ Hubbard model, we obtain in the MF the expected long-range anti-ferromagnetic (AFM)

Neel order at a transition temperature, T_N^{mf} , which is associated with the occurrence of a gap Δ^{mf} in the spectrum. When fluctuation effects are incorporated through the SCR scheme, the Neel transition is suppressed so that $T_N \rightarrow 0$, consistent with the Mermin-Wagner theorem,⁶ but a pseudogap Δ^* tied to the appearance of *short-range* AFM correlations turns on near a temperature T^* . We find in particular that $\Delta^* \simeq \Delta^{mf}$ and $T^* \simeq T_N^{mf}$. In other words, the MF values Δ^{mf} and T_N^{mf} can be viewed as being representative of the *pseudogap and its onset* in the two-dimensional (2D) Hubbard case.^{7,8} This is a key observation suggested by our SCR and MF analysis. Incidentally, when we include interlayer hopping in our Hamiltonian, a finite T_N is restored with little effect on Δ^* if $T_N \ll T^*$, which is the case here. Hence Δ^* and T_N get decoupled, even though the MF solution incorrectly couples these two quantities.⁹

Another aspect which bears emphasis is that for *hole doping* the AFM solution obtained in the MF is unstable towards the formation of incommensurate phases or phase separation.^{10,11} In sharp contrast, we find that in the *electron-doped* case the MF and SCR solutions do not show such an instability. These results indicate that the MF solution—when interpreted properly along the lines of the preceding paragraph—can be remarkably valuable in describing the electron-doped cuprates.

With this motivation, we focus now on the presentation and interpretation of the MF results. Our one-band Hubbard model is defined by the independent particle dispersion $\epsilon_{\mathbf{k}} = -2t(c_x + c_y) - 4t'c_xc_y - 4t''(c_x^2 + c_y^2 - 1)$, with $c_i = \cos k_i a$ and lattice constant a . The band parameters are taken to be $t=0.326$ eV, $t'=-0.25t$, $t''=0.1t$, independent of doping.¹² On-site repulsion U is treated as a doping-dependent effective parameter $U_{eff}(x)$, with $U_{eff}(0)=6t$. For the half-filled case ($x=0$), the preceding values are generally consistent with earlier $t-J$ and $t-U$ model calculations.¹³⁻¹⁵

The Mott gap Δ^{mf} is well known to arise in the MF (using spin-density-wave treatment¹⁶) from a finite expectation value of the staggered magnetization $m_{\mathbf{Q}}$ at wave vector $\mathbf{Q}=(\pi, \pi)$. The energy spectrum then consists of an upper Hubbard band (UHB), which is empty at half-filling, and a lower Hubbard band (LHB) (Ref. 17) given by

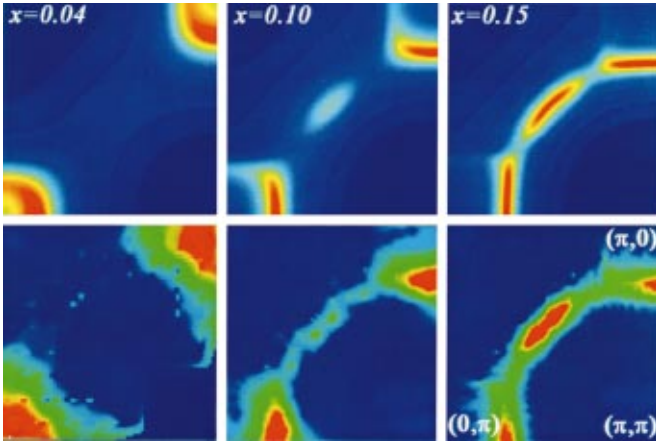


FIG. 1. (Color) Top row: Theoretical FS maps in NCCO for different dopings x , obtained by integrating the spectral density function (see Eq. 3) over an energy window of 60 meV around E_F ; highs denoted by red and lows by blue. Bottom row: Corresponding experimental maps after Ref. 1.

$$E_{\mathbf{k}}^{U,L} = (\epsilon_{\mathbf{k}} + \epsilon_{\mathbf{k}+\mathbf{Q}} \pm E_{0\mathbf{k}})/2 \quad (1)$$

$$1 = U \sum_{\mathbf{k}} [f(E_{\mathbf{k}}^L) - f(E_{\mathbf{k}}^U)]/E_{0\mathbf{k}}, \quad (2)$$

where the $+$ ($-$) sign refers to the UHB(LHB); the gap between UHB and LHB is $2\Delta^{mf}$. Here, $E_{0\mathbf{k}} = [(\epsilon_{\mathbf{k}} - \epsilon_{\mathbf{k}+\mathbf{Q}})^2 + 4(\Delta^{mf})^2]^{1/2}$, and f is the Fermi function. We solve Eqs. 1 and 2 self-consistently as a function of electron doping such that the computed value of Δ^{mf} equals the experimentally observed value of the pseudogap which yields $U_{eff}(x)$ as a function of x . The single-particle Green function is

$$G(\mathbf{k}, E) = u_{\mathbf{k}}^2 [E - E_{\mathbf{k}}^U]^{-1} + v_{\mathbf{k}}^2 [E - E_{\mathbf{k}}^L]^{-1}, \quad (3)$$

where the weights or ‘‘coherence’’ factors of states in the UHB and LHB are $u_{\mathbf{k}}^2 = 1 - v_{\mathbf{k}}^2 = (1 + (\epsilon_{\mathbf{k}} - \epsilon_{\mathbf{k}+\mathbf{Q}})/2E_{0\mathbf{k}})/2$. Equation 3 allows the computation of the spectral density $A(\mathbf{k}, E)$ via $\text{Im}[G(\mathbf{k}, E)]$. The FS maps are obtained from

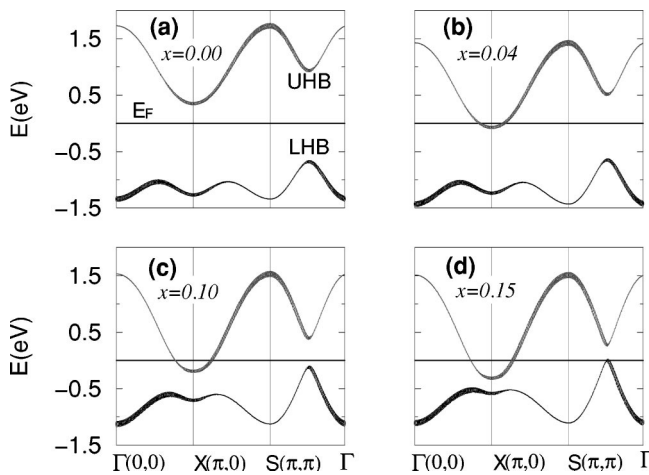


FIG. 2. Dispersions of UHB and LHB for various dopings x . E_F defines the energy zero. Spectral weights (see Eq. 3) are given by thickness of bands.

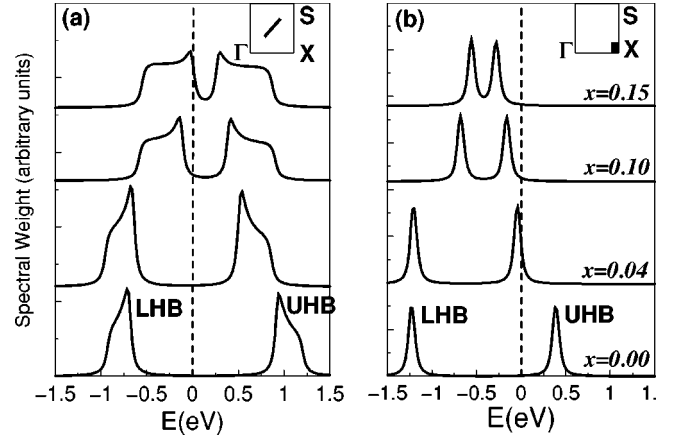


FIG. 3. Integrated spectral weight around (a) $(\pi/2, \pi/2)$, and (b) $(\pi, 0)$ points, for four different doping levels, x . Insets give the \mathbf{k} regions over which the spectral weight was integrated. E_F defines the energy zero.

$A(\mathbf{k}, E_F)$ with energy fixed at the Fermi energy E_F . These theoretical FS emission maps do not account for the effects of the ARPES matrix element⁵—a point to which we return below.

Figure 1 compares theoretical (top row) and experimental¹ (bottom row) evolution of the FS with doping. The agreement is seen to be remarkable: At low doping ($x = 0.04$), both sets of maps show the appearance of small FS pockets centered at $(\pi, 0)$ and $(0, \pi)$; With increasing doping ($x = 0.10$), these pockets begin to look squarish in shape with half of the square losing much of its intensity, and additionally, a pocket begins to form around $(\pi/2, \pi/2)$ and weak intensity appears around the magnetic Brillouin zone (BZ) boundary [diagonal line joining the $(\pi, 0)$ and $(0, \pi)$ points]; Finally, at $x = 0.15$, the $(\pi/2, \pi/2)$ pocket is well formed and the three pieces of the FS, when viewed together, begin to resemble a single large (π, π) -centered FS sheet displaying ‘‘hot-spots’’¹⁸ (points of intersection of FS with the BZ diagonal).

Insight into this FS evolution is provided by the dispersions of the UHB and LHB in Fig. 2. The linewidths depict spectral weights of various k states in Eq. 3. E_F is seen to

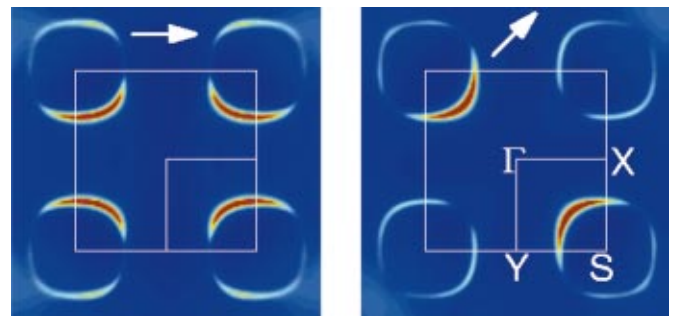


FIG. 4. (Color) Theoretical FS maps in NCCO obtained via first principles simulations which include the effect of the ARPES matrix element but not of strong correlations for two different polarizations (white arrows) at a photon energy of 16 eV. Color scheme as in Fig. 1.

shift smoothly into the UHB with increasing doping. At low doping, in Fig. 2(b), E_F lies above the band minimum in the UHB at X and gives rise to the $(\pi,0)$ -centered electron pocket¹⁹ with a symmetrical pocket at $(0,\pi)$. At $x=0.10$, in Fig. 2(c), the intersection of E_F with the UHB is seen to have little weight along the $\Gamma-X$ line, but a large spectral weight along $X-S$, thereby explaining how one-half of the $(\pi,0)$ electron pocket loses intensity at the expense of the other half as noted in connection with Fig. 1 above. Moreover, in Fig. 2(c), the cusp in the LHB near $(\pi/2,\pi/2)$ (located slightly closer to Γ on the $\Gamma-S$ line) lies within the experimental resolution of Ref. 1 and begins to yield intensity. At $x=0.15$, the $(\pi/2,\pi/2)$ hole pocket is well formed, but the k states in one-half of this pocket possess relatively little weight and the thick portions of the UHB and LHB resemble the uncorrelated band structure, the presence of a small residual gap notwithstanding. These theoretical dispersions are in reasonable accord with the measurements, which are limited at the moment mostly to the LHB around the $(\pi/2,\pi/2)$ and $(0,\pi)$ region.¹ Also, in this doping regime, transport studies find evidence for two-band conduction and a change in the sign of the Hall coefficient;²⁰ the hole pocket associated with the LHB can explain both these effects.

The energy dependence of spectral weights in the vicinity of the $(\pi/2,\pi/2)$ and $(\pi,0)$ points is considered in Fig. 3. At $(\pi/2,\pi/2)$ in Fig. 3(a), LHB and UHB lie below and above E_F respectively at low doping, but shift rapidly towards E_F with increasing doping. Since ARPES only sees states below E_F , the results of Fig. 3(a) are in accord with the corresponding ARPES data [see Fig. 2(a) of Ref. 1] where the spectral weight is seen to move from a binding energy of 1.3 eV to 0.3 eV in going from $x=0$ to $x=0.15$. The behavior of spectra differs sharply at $(\pi,0)$ in Fig. 3(b). Here, at low doping, UHB lies at E_F while the LHB lies well below E_F . With increasing doping, the LHB rapidly moves towards E_F , but the UHB slowly moves to lower energy. In the corresponding ARPES data [see Fig. 2(b) of Ref. 1], an increase in the spectral weight in the vicinity of E_F is seen much like the results of Fig. 3(b), suggesting that electrons first enter the UHB at the $(\pi,0)$ point.

In order to ascertain whether the FS features of Fig. 1 could be caused by effects of the ARPES matrix element,⁵ we have carried out extensive first-principles simulations of the ARPES intensities in NCCO based on the conventional LDA-based band theory framework where the ARPES matrix element is properly treated and the photoemission process is modeled by including full crystal wave functions in the presence of the surface.^{5,21} A variety of photon energies, polarizations, and surface terminations were sampled. The computed FS maps for the Nd-CuO₂-Nd-O₂-terminated surface at 16 eV shown in Fig. 4 for two different polarizations are typical. The intensity is seen to undergo large variations around the $S(\pi,\pi)$ centered hole orbit, and to nearly vanish along certain high symmetry lines in some cases. Nevertheless, we do not find any situation which resembles the doping dependencies displayed in Fig. 1. It is clear that strong correlation effects beyond the conventional LDA-based picture

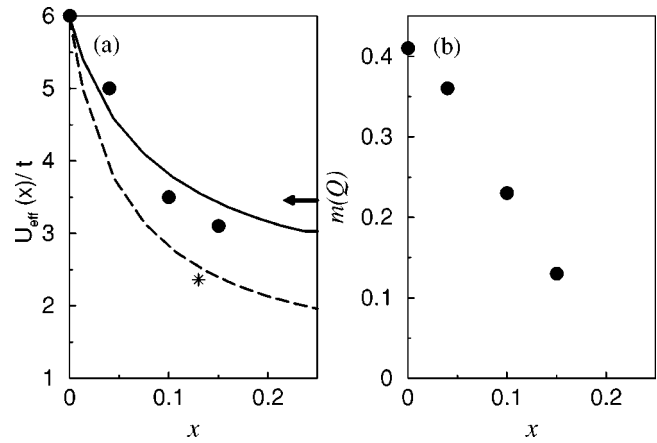


FIG. 5. (a) Various calculations of $U_{eff}(x)$: Values from a screened computation (see text) for electrons (solid lines) and holes (dashed lines); filled circles: this work; arrow, Kanamori (Ref. 22); star, Monte Carlo studies (Ref. 23,24). (b) Staggered magnetization $m_Q(x)$ for present computations.

are needed to describe the experimental ARPES spectra and that the $t-t'-t''-U$ Hubbard model captures some of the essential underlying physics.

Figure 5(a) compares the x dependence of $U_{eff}(x)$ found in the current study (solid dots) with various estimates given in the caption.²²⁻²⁴ We have also carried out a computation of $U_{eff}(x)$ where the bare $U=6.75t$ was screened using, $U_{eff}=U/(1+\langle P \rangle U)$, via the charge susceptibility P . The U_{eff} so obtained for electrons (solid line) as well as holes (dashed) is shown. Figure 5(a) clearly shows that the weakening of U_{eff} with increasing doping adduced in this work—one of our key results—is consistent with a number of other calculations and models.²⁵

The x dependence of the staggered magnetization, $m_Q(x)$, shown in Fig. 5(b), is interesting. $m_Q(x)$ and hence the pseudogap ($\propto m_Q(x)$) is seen to vanish slightly above optimal doping where the $T=0$ Neel ordered phase also terminates, yielding a QCP.²⁶ Notably, superconductivity near an AFM QCP has been reported in a number of systems²⁷—including the hole-doped cuprates.²⁸

For hole doping, however, the FS evolution follows a very different route. In the one-band Hubbard model²⁹ holes first enter the LHB as small hole pockets around $(\pi/2,\pi/2)$. However, as already noted,¹⁰ the uniformly doped AFM state is unstable and leads to complications of (nanoscale) phase separation and stripe physics not expected for electron doping¹¹. Indeed, characteristic experimental signatures of stripe order, e.g., the $1/8$ anomaly and the NQR wipeout, appear greatly attenuated if not absent in NCCO,³⁰ and E_F shifts smoothly with doping into the UHB.³¹ Despite these differences, the pseudogap and *short-range* AFM order collapse in a QCP at a very similar doping level with hole or electron doping,^{28,32} although in hole-doped cuprates interpretation of the pseudogap is ambiguous both because the UHB lies above E_F and because there are competing orders capable of inducing spectral gaps.⁸

A crossover from small to large FS has been studied before using slave bosons for the $t-J$ models,¹⁹ but the inti-

mate connection with the Mott pseudogap collapse has not previously been noted. Indeed, the $t-J$ class of models, which simplifies the problem by assuming that U is so large that one Hubbard subband can be neglected, will have difficulty whenever the two subbands approach, and can only analyze this situation with additional parameters or by reintroducing U . Hence, a model which works directly with U obtains considerable advantage.³³

In conclusion, this study indicates that electron doped NCCO is an ideal test case for investigating how the Mott gap evolves with doping in a Mott insulator, untroubled by

complications of stripe phases. The doping dependence of U_{eff} adduced in this work has implications in understanding the behavior of cuprates more generally since the pseudogap in both the electron and the hole doped systems must arise from the same fundamental gap at sufficiently low doping.

We thank N. P. Armitage and Z. -X. Shen for sharing their data with us prior to publication. This work was supported by the U.S. DOE Contract No. W-31-109-ENG-38 and benefited from the allocation of supercomputer time at the NERSC and the Northeastern University Advanced Scientific Computation Center (NU-ASCC).

-
- ¹N.P. Armitage *et al.*, Phys. Rev. Lett. **87**, 147003 (2002).
²A three-band model gives very similar results (Ref. 4).
³T. Moriya, *Spin Fluctuations in Electron Magnetism* (Springer, Berlin, 1985).
⁴R.S. Markiewicz (unpublished).
⁵A. Bansil and M. Lindroos, Phys. Rev. Lett. **83**, 5154 (1999); M. Lindroos and A. Bansil, *ibid.* **75**, 1182 (1995).
⁶N.D. Mermin and H. Wagner, Phys. Rev. Lett. **17**, 1133 (1966).
⁷We refer to Δ^{mf} as a Mott pseudogap since it arises from correlation effects in the spirit of the Mott-Hubbard metal-insulator transition. We do not address disorder related localization effects away from half filling.
⁸There are many other views on the origin of pseudogap in the cuprates (superconducting fluctuations, etc.). See, e. g., R.S. Markiewicz, cond-mat/0108075, Phys. Rev. Lett. (to be published); S. Andergassen *et al.*, Phys. Rev. Lett. **87**, 056401 (2001).
⁹MF is often considered seriously deficient due to the large value of T_N^{mf} . See, e. g., J. Brinkmann and P.A. Lee, Phys. Rev. B **65**, 014502 (2001).
¹⁰A. Singh and Z. Tešanović, Phys. Rev. B **41**, 614 (1990); A.V. Chubukov and D.M. Frenkel, *ibid.* **46**, 11 884 (1992); C. Zhou and H.J. Schulz, *ibid.* **52**, 11 557 (1995).
¹¹R.S. Markiewicz and C. Kusko, Phys. Rev. B **65**, 064520 (2002).
¹²Even without including the small t'' , we obtain quite good agreement with experiment.
¹³R.S. Markiewicz, Phys. Rev. B **62**, 1252 (2000).
¹⁴C. Kim *et al.*, Phys. Rev. Lett. **80**, 4245 (1998).
¹⁵Optimal values of t' , t'' differ slightly in $t-U$ and $t-J$ models [Tohyama *et al.*, J. Phys. Soc. Jpn. **69**, 9 (2000)], former values are more relevant here.
¹⁶J.R. Schrieffer *et al.*, Phys. Rev. B **39**, 11 663 (1989).
¹⁷LHB yields the Zhang-Rice singlet in the three-band case.
¹⁸R. Hlubina and T.M. Rice, Phys. Rev. B **51**, 9253 (1995); N.P. Armitage *et al.*, Phys. Rev. Lett. **87**, 147003 (2001).
¹⁹ $(0,\pi)$, $(\pi,0)$ pockets have been noted in the $t-J$ model by T. Tohyama and S. Maekawa Phys. Rev. B **64**, 212505 (2001).
²⁰M. Suzuki *et al.*, Phys. Rev. B **50**, 9434 (1994); W. Jiang *et al.*, Phys. Rev. Lett. **73**, 1291 (1994).
²¹M. Lindroos, S. Sahrakorpi, and A. Bansil, Phys. Rev. B **65**, 054514 (2002); A. Bansil *et al.*, *ibid.* **60**, 13 396 (1999).
²²J. Kanamori, Prog. Theor. Phys. **30**, 275 (1963).
²³N. Bulut *et al.*, Phys. Rev. B **47**, 2742 (1993).
²⁴L. Chen *et al.*, Phys. Rev. Lett. **66**, 369 (1991).
²⁵In SCR analysis, there is an additional correction due to quantum renormalization of the AFM Stoner criterion, $\chi_0 U_{eff} = \eta > 1$, with χ_0 the bare susceptibility.
²⁶Inclusion of fluctuations via SCR drives T_N and the *long-range* m_Q to zero, but there is still *short-range* magnetization and a (somewhat shifted) QCP, now associated with termination of the $T=0$ Neel order.
²⁷N.D. Mathur *et al.*, Nature (London) **394**, 39 (1998).
²⁸J.L. Tallon *et al.*, Phys. Status Solidi B **215**, 531 (1999).
²⁹A.V. Chubukov and D.K. Morr, Phys. Rep. **288**, 355 (1997).
³⁰M. Ambai *et al.*, J. Phys. Soc. Jpn. **71**, 538 (2002).
³¹N. Harima *et al.*, Phys. Rev. B **64**, 220507 (2001).
³²This suggests the importance of phase separation effects in suppressing Neel order, and explaining why T_N falls off so much faster with hole vs electron doping. This point will be taken up further elsewhere.
³³Note that in the $t-J$ models the bands are inverted for treating electron doping, leading to a sign change of t' which is not needed in the $t-U$ models.